

Combined in-situ small and wide-angle synchrotron X-ray scattering (SAXS–WAXS) applied to a solid-state polymerization reaction

Oliver Herzberg^a, Rainer Gehrke^b, Matthias Eppe^{a,*}

^a*Institute of Inorganic and Applied Chemistry, University of Hamburg, Martin-Luther-King-Platz 6, D-20146 Hamburg, Germany*

^b*Hamburger Synchrotronstrahlungslaboratorium (HASYLAB) am Deutschen Elektronensynchrotron (DESY), Notkestr. 85, D-22603 Hamburg, Germany*

Received 17 February 1998; revised 21 April 1998

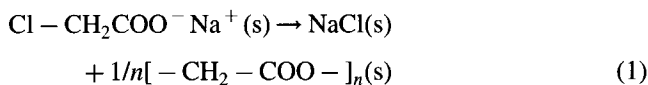
Abstract

The solid-state elimination reaction in sodium chloroacetate was studied with in-situ combined small- and wide-angle X-ray scattering (SAXS–WAXS). This reaction leads to sodium chloride cubes ($d \approx 1 \mu\text{m}$) finely dispersed in a matrix of partially crystalline polyglycolide, poly(hydroxyacetic acid). The wide-angle data confirm a single-step reaction without detectable intermediate. The formation of the superstructure of polyglycolide (detectable by SAXS) is delayed compared to the formation of crystalline domains (detectable by WAXS). This is indicated by the intensity of the long period diffraction peak at $s = 0.104 \text{ nm}^{-1}$. © 1998 Elsevier Science Ltd. All rights reserved.

Keywords: Solid-state polymerization; Small-angle scattering; Biodegradable

1. Introduction

The elimination reaction in halogenoacetates has been known for more than 140 years [1,2]. We have reported detailed studies of this reaction with modern physicochemical methods and found that it occurs as a solid-state reaction without detectable intermediate [3–7]:



Sodium chloride cubes with sizes in the micrometer range and below (0.2–1.5 μm) are formed within a matrix of polyglycolide. After having studied this reaction type on different halogenoacetates with various solid-state chemical techniques, it was of interest to employ a method that is more sensitive to the properties of the formed polymer. Small-angle scattering provides insight into a size region that is neither accessible by common diffraction techniques nor by scanning electron microscopy. Taking that into account, we have carried out the above reaction using simultaneous small- and wide-angle X-ray scattering, making full advantage of the high intensity of synchrotron radiation. This permits in-situ experiments that give better insight into dynamic systems than ex-situ studies on quenched aliquots [8].

2. Experimental

Sodium chloroacetate was prepared from sodium hydroxide and chloroacetic acid and purified by recrystallization from ethanol. It was characterized by elemental analysis, i.r. spectroscopy, ¹H and ¹³C n.m.r. spectroscopy, X-ray powder diffraction and differential scanning calorimetry.[4] Most alkali salts of halogenoacetic acids undergo the desired solid-state polymerization reaction; however, sodium chloroacetate was chosen as suitable reference substance because of comparatively small absorption of the X-ray beam by the sample.

Combined small- and wide-angle X-ray scattering experiments (SAXS–WAXS) were carried out at HASYLAB at DESY at beamline A2 [9]. At this beamline simultaneous SAXS–WAXS experiments are possible in transmission geometry. The X-ray wavelength was 1.54 Å. The lower half of the scattered beam was directed to the WAXS-detector, the upper half was directed to the SAXS-detector. Linear position-sensitive detectors (PSDs) with 512 channels each were used. The data collection time was 2 min for a pair of frames. The PSD readouts were calibrated with the signals of NaCl, polyethylene terephthalate (PET) and sodium chloroacetate for WAXS and rat-tail collagen (long period: 65 nm) for SAXS.

The sample was pressed into a thin pellet (thickness about 0.5 mm) and covered with aluminium foil on both sides to avoid disintegration during heating, and to improve the

* Corresponding author.

temperature homogeneity. The copper-made furnace was heated electrically and cooled with pressurized air. The sample chamber was kept under static air atmosphere while the remainder of the beam path was evacuated. The beam path in air was about 2 cm. The temperature was taken with a thermocouple near the sample. It was possible to simultaneously access a SAXS region in $s = 1/d = (2 \cdot \sin\Theta)/\lambda$ of $0.022\text{--}0.200 \text{ nm}^{-1}$ (s is the scattering vector defined as the reciprocal lattice spacing, d the lattice spacing, Θ the scattering angle, and λ the X-ray wavelength) and a WAXS region in 2Θ of $16\text{--}35^\circ$.

The data evaluation was performed with self-programmed routines. After calibration for 2Θ and s , respectively, the intensity was corrected for the primary beam intensity decay. The background scatter due to air, sample holder and aluminium was removed by subtracting the diffractogram of a reference double-aluminium foil.

3. Results and discussion

The techniques that were applied in earlier studies were mainly sensitive to the inorganic part of the molecule, i.e., the halogen or the metal: X-ray absorption spectroscopy (EXAFS) can trace halogenoacetate and metal halide, [3,5,10] and XRD detects mainly the well-crystallized phases, i.e. again halogenoacetate and metal

halide [3,5]. The crystalline fraction of polyglycolide is detected in XRD, but the reflections are difficult to quantify besides the strongly scattering and absorbing metal halide phases. i.r. spectroscopy yields more qualitative structural information [11]. Therefore, little is known yet about the reaction pathway of the polymer from its initial stages as nucleus to the final bulk form.

A very useful technique in polymer chemistry is small-angle X-ray scattering (SAXS). If the technique is applied in situ, thermally induced phase changes like recrystallizations can be monitored and quantitatively interpreted [9,12–15]. In situ small-angle X-ray scattering has been combined with wide-angle scattering (i.e., conventional X-ray diffractometry) [9,16–18]. In such a SAXS–WAXS set-up, all crystalline phases can be identified and quantified by means of their characteristic diffraction peaks. Additionally, set-ups have been realized where the SAXS-signal is monitored simultaneously with a d.s.c. signal (SAXS–d.s.c.) [19–21], sometimes even together with the WAXS signal (SAXS–WAXS–d.s.c.) [9,22,23]. These developments have been greatly enhanced, especially in the polymer field, by the intense synchrotron radiation [9,12–14].

A sample of sodium chloroacetate was heated within 2 min from room temperature to 180°C and kept for 60 min at this temperature. SAXS and WAXS patterns were recorded simultaneously every 2 min.

The in situ recorded SAXS scans are shown in Fig. 1. The evolution of the polyglycolide long period peak at $s \approx$

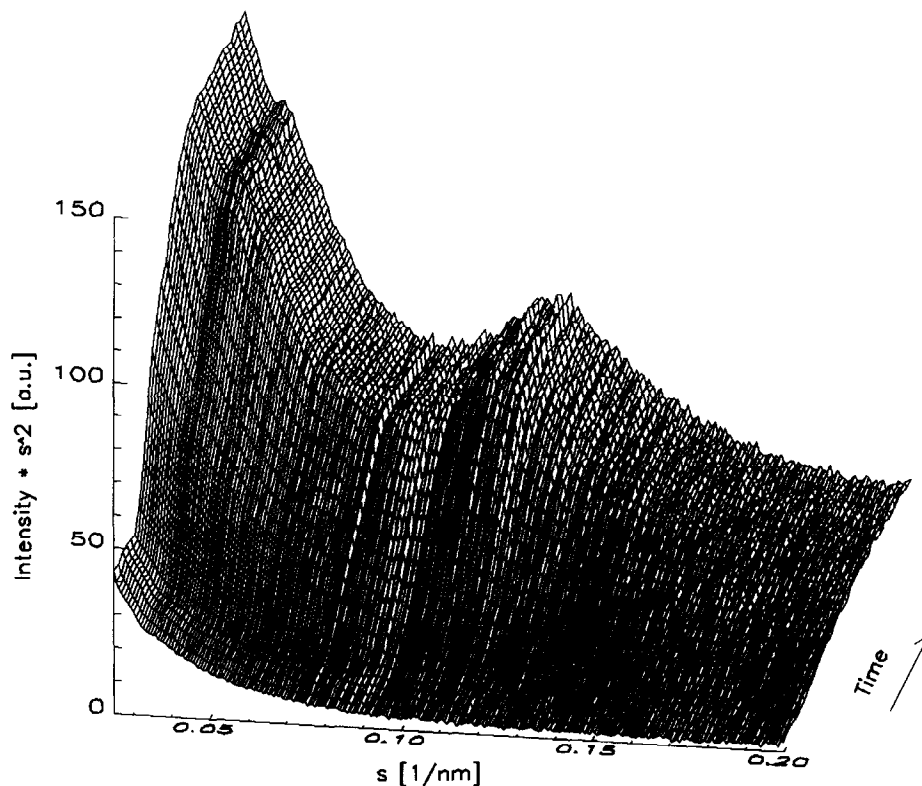


Fig. 1. Pseudo three-dimensional representation of small-angle X-ray scattering curves (SAXS) recorded for 60 min at 180°C during the elimination reaction of sodium chloroacetate.

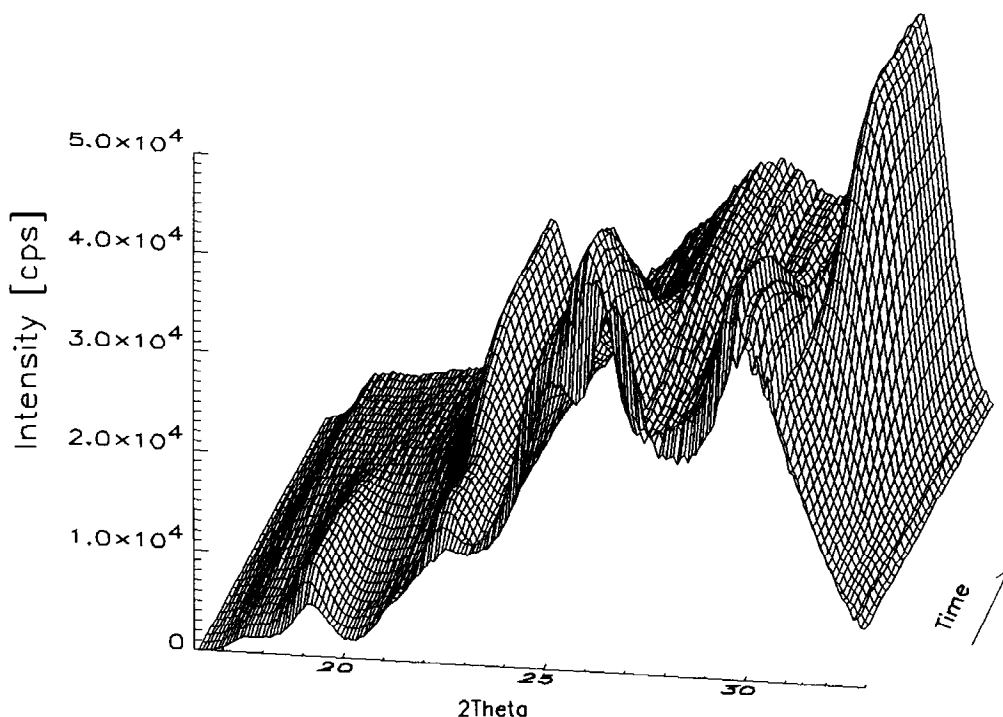


Fig. 2. Pseudo three-dimensional representation of wide-angle X-ray scattering curves (WAXS) recorded during the reaction of sodium chloroacetate (60 min isothermal annealing at 180°C). Characteristic peaks: sodium chloroacetate at 19, 22, 26 and 30°2 θ ; sodium chloride at 32°2 θ ; polyglycolide at 22 and 26°2 θ .

0.1 nm⁻¹ and the increase in scattering power are easily seen.

In the wide-angle region (WAXS), distinct structural changes from sodium chloroacetate to sodium chloride and partially crystalline polyglycolide occur (Fig. 2). The formed polyglycolide is of considerable crystallinity as indicated by the strong reflections at 22°(011) and 26°2 θ (200). As the instrument is not designed to give high-resolution WAXS diagrams, peak widths are larger than those encountered in conventional powder diffraction. This leads to strong overlap and a 'mountain' in intensity between 22° and 32°2 θ . In conventional XRD, the amorphous halo was comparatively small, therefore it is expected to be negligible here as well. No peaks of intermediate compounds can be detected.

Fig. 3 shows the SAXS patterns of the parent compound sodium chloroacetate at the start of the experiment and of the reaction product polyglycolide/NaCl after 60 min at 180°C. It is obvious that the total scattering power has increased considerably during the reaction. Additionally, a Bragg peak has appeared at $s = 0.104$ nm⁻¹, corresponding to a d -value of ca. 96 Å (9.6 nm). This is attributed to the long-period L of polyglycolide, in reasonable agreement with data obtained by other authors. Polyakov et al. found 60.5 Å for polyglycolide prepared from sodium chloroacetate and 72.2 Å for polyglycolide prepared by ring-opening polymerization of glycolide [24]. SAXS on polyglycolide- ϵ -caprolactone diblock copolyesters (prepared in solution) gave long-periods between 108 and 155 Å [25]. These were interpreted in terms of a micellar structure with crystalline polyglycolide segments surrounded by ϵ -caprolactone blocks. The appearance of this

diffraction peak indicates a well-developed superstructure of the formed polyglycolide.

It can be easily understood that the total scattering power increases during the reaction. As many small salt microcrystals are formed during the reaction, we have a high degree of heterogeneity in the system, and many small particles that are able to scatter the X-radiation. Additional scattering is caused by density differences between amorphous and crystalline polyglycolide.

Besides these more qualitative impressions, a quantitative evaluation of both SAXS and WAXS data was carried out. Let us first consider the SAXS results.

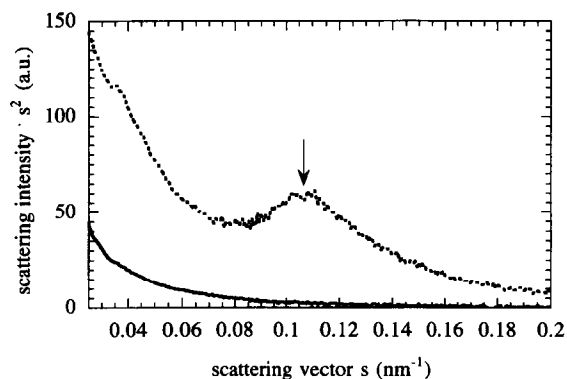


Fig. 3. Small-angle X-ray scattering curves (SAXS) of the starting compound sodium chloroacetate (solid line) and the reaction product polyglycolide + sodium chloride after 60 min at 180°C (dashed line). The broad peak at $s = 0.104$ nm⁻¹ is attributed to the long-period L of the formed polyglycolide.

A measure of the total scattering power is the Porod invariant [26], defined as

$$Q = 4\pi \int_{s_{\min}}^{s_{\max}} I(s) \cdot s^2 ds \quad (2)$$

with $I(s)$ the scattered intensity at the scattering vector s .

Ideally, s should range from 0 to infinity. As the complete range in s is generally not accessible, we used a suitable range from the beam-stop (= maximum of the scattering curve) to the highest measured s . Note that the invariant should not include the wide-angle diffraction peaks. Practically, the intensity approaches zero soon at higher scattering vectors (s 0.25 nm⁻¹). In this case, a range in s of 0.025 to 0.2 nm⁻¹ was used throughout all scans. Fig. 5 contains the change in Q with time.

For a two-phase system of two components 1 and 2, the invariant Q is given by

$$Q = K \cdot \nu_1 \cdot \nu_2 \cdot |\rho_1 - \rho_2|^2 = K \cdot \nu_1 \cdot (1 - \nu_1) \cdot |\Delta\rho|^2 \quad (3)$$

where ν_1 and ν_2 are the volume fractions and ρ_1 and ρ_2 the densities of components 1 and 2, respectively. K is a constant dependent on the system and the experimental conditions. For a system consisting of four components with different density as encountered here (sodium chloroacetate, sodium chloride, crystalline polyglycolide, amorphous polyglycolide) the simple relationship of Eq. 3 is not valid. However, given the substantial information about the morphology reported above, the increase in Q can be interpreted as increasing heterogeneity as the sample changes from pure sodium chloroacetate to sodium chloride finely dispersed in a matrix of partly crystalline polyglycolide.

A quantitative evaluation of the diffraction peaks in both SAXS and WAXS is shown in Fig. 4. The peaks have been

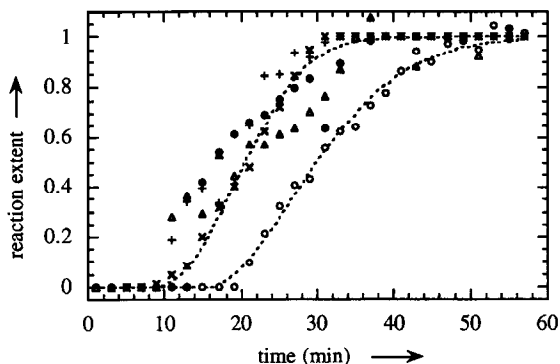


Fig. 4. Small- and wide-angle X-ray scattering on sodium chloroacetate: Normalized peak intensities as a function of time, converted to the reaction extent α . Suitable functions have been fitted to the curves for the four WAXS peaks and the SAXS peak. The evolution of the SAXS peak is delayed compared to the four WAXS peaks; \circ SAXS: Polyglycolide long period L at 0.104 nm⁻¹: $\alpha = I(t)/I(t = \infty)$; \times WAXS: Sodium chloroacetate peak at 18.9°2 θ : $\alpha = 1 - I(t)/I(t = \infty)$; $+$ WAXS: Sodium chloroacetate peak at 29.7°2 θ : $\alpha = 1 - I(t)/I(t = \infty)$; \bullet WAXS: Polyglycolide (011) peak at 22.2°2 θ : $\alpha = I(t)/I(t = \infty)$; \blacktriangle WAXS: Sodium chloride (200) peak at 31.8°2 θ : $\alpha = I(t)/I(t = \infty)$.

corrected for background scattering, decomposed by peak fitting and fitted with asymmetric profiles. The accuracy of the wide-angle data is only moderate, as the peaks are generally broad and overlapped. This made background subtraction and decomposition difficult. It was no problem to extract the diffraction peak corresponding to the long period L from the SAXS data. A proportionality between peak intensity ratio and reaction extent α is valid as no mass loss occurs during this reaction [27].

All diffraction peaks from WAXS follow the same α/t -curve within the experimental scatter. This is in good agreement with earlier results, showing that no crystalline intermediate occurs.

However, the evolution of the long period diffraction peak is delayed compared with the WAXS data. The time lag is about 5–10 min, and it appears as if the growth of this peak is not even completed at the end of the experiment. This is interpreted as follows: When polyglycolide is formed by solid-state reaction, it is precipitated in small particles. Soon the particles reach a size which shows coherent Bragg scattering, as shown by the distinct diffraction peaks in WAXS, and continue to grow. However, the formation of the superstructure that is responsible for the occurrence of a diffraction peak of the long period requires larger particles and also some assembling and ordering of crystalline and amorphous regions. This explains why the SAXS peak at 0.104 nm⁻¹ is delayed. This process is not finished with the ‘chemical’ completion, but appears to continue during further annealing.

It should be mentioned that neither the position nor the width of the long period diffraction peak change with time within the experimental scatter. Therefore, it can be stated that the superstructure remains constant throughout the experiment within the detection limit. As the NaCl crystals are almost all larger than 200 nm [6], small-angle scattering by the dispersed NaCl is ruled out. Note that the formation of crystalline polyglycolide cannot be directly compared to the crystallization of molten polymers [28], as the product

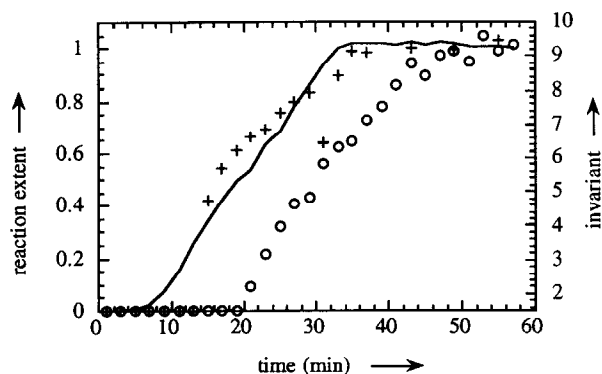


Fig. 5. Compilation of the characteristic data obtained by in situ SAXS–WAXS for the solid-state polymerization of sodium chloroacetate. $\circ \circ \circ$ SAXS: Long period L at 0.104 nm⁻¹: $\alpha = I(t)/I(t = \infty)$; $+$ WAXS: Polyglycolide (011) peak at 22.2°2 θ : $\alpha = I(t)/I(t = \infty)$; — SAXS: Porod invariant (total scattering power).

that is to crystallize is not present at the beginning of the experiment but formed during it.

These conclusions are summarized in Fig. 5, where the characteristic data for polyglycolide are compiled. The relationship between the formation of crystalline polyglycolide (and thereby NaCl) and the scattering invariant is obvious. Additionally, the delayed development of the polyglycolide superstructure can be seen.

Further experiments with a constant heating rate confirmed these isothermal results. The sample was also monitored during cooling from 200°C to 25°C, followed by renewed heating, and a reversible decrease in the invariant was observed. This is attributed to decreasing density differences between NaCl and polyglycolide phases upon cooling. This density change had a similar effect on the integrated intensity of the long period diffraction peak: its intensity increased with rising temperature due to an increasing density difference between crystalline and amorphous polyglycolide [28].

4. Conclusions

These results complement those presented in earlier communications, as with the SAXS technique more information about the behaviour of the formed polyglycolide could be obtained. Consumption of sodium chloroacetate occurs simultaneously with the formation of sodium chloride and crystalline polyglycolide. This confirms a single-step solid-state reaction. However, ordering processes in the polymer, i.e. the evolution of a superstructure (as detectable in SAXS) occur delayed, compared to the formation of crystalline polyglycolide and NaCl (as detectable in WAXS). This underscores the complexity of reacting solids, where changes can still occur when the reaction is 'chemically finished'. Very similar observations have been made with in-situ X-ray diffraction that showed that the formed salt crystals continue to grow after the reaction is chemically finished [5].

Acknowledgements

We thank the staff at beamline A2 for experimental

support and Dr. N. Stribeck, Hamburg, for helpful discussions. We thank Prof. A. Reller for continuous support. We are grateful to the late Prof. H.G. Zachmann for helping to initiate this study. This work was supported by the Fonds der Chemischen Industrie and the Deutsche Forschungsgemeinschaft. We thank HASYLAB at DESY for generous allocation of beam-time.

References

- [1] Hoffmann R. *Liebigs Ann Chem* 1857;102:1.
- [2] Kekulé A. *Liebigs Ann Chem* 1858;105:288.
- [3] Epple M, Tröger L. *J Chem Soc Dalton Trans* 1996;11.
- [4] Epple M, Kirschnick H. *Chem Ber* 1996;129:1123.
- [5] Epple M, Sankar G, Thomas JM. *Chem Mater* 1997;9:3127.
- [6] Epple M, Herzberg O. *J Mater Chem* 1997;7:1037.
- [7] Elizabé L, Kariuki BM, Harris KDM, Tremayne M, Epple M, Thomas JM. *J Phys Chem B* 1997;101:8827.
- [8] Epple M. *J Therm Anal* 1994;42:559.
- [9] Zachmann HG. *Nucl Instrum Meth* 1995;B97:209.
- [10] Epple M, Sazama U, Reller A, Hilbrandt N, Martin M, Tröger L. *J Chem Soc Chem Commun* 1996;1755.
- [11] Epple M, Kirschnick H, Thomas JM. *J Therm Anal* 1996;47:331.
- [12] Gehrke R. *Topics Curr Chem* 1989;151:111.
- [13] Riekel C. *Topics Curr Chem* 1989;151:205.
- [14] Ryan AJ, Elwell MJ, Bras W. *Nucl Instrum Meth* 1995;B97:216.
- [15] Stein RS, Cronauer J, Zachmann HG. *J Mol Struct* 1996;383:19.
- [16] Ryan AJ. *J Therm Anal* 1993;40:887.
- [17] Oversluizen M, Bras W, Greaves GN, Clark SM, Thomas JM, Sankar G, Tiley B. *Nucl Instrum Meth* 1995;B97:184.
- [18] Butler MF, Donald AM, Bras W, Mant GR, Derbyshire GE, Ryan AJ. *Macromolecules* 1995;28:6383.
- [19] Koberstein J, Russell TP. *Macromolecules* 1986;19:714.
- [20] Bras W, Derbyshire GE, Devine A, Clark SM, Cooke J, Komanschek BE, Ryan AJ. *J Appl Cryst* 1995;28:26.
- [21] Androsch R, Stolp M, Radosch HJ. *Thermochim Acta* 1996;271:1.
- [22] Bark M, Zachmann HG. *Acta Polym* 1993;44:259.
- [23] Haswell R, van Mechelen JB, Mensch CTJ, de Groot H. *Nucl Instrum Meth* 1995;B97:242.
- [24] Zhubov YA, Selikhova VI, Shirets VS, Chebotareva IA, Polyakov DK. *Vysokomolekulyarne soedineniya Seriya A and Seriya B* 1995;37:1784.
- [25] Sobry R, Vandebossche G, Fontaine F, Barakat I, Dubois P, Jerome R. *J Mol Struct* 1996;383:63.
- [26] Porod G. *Coll Polym Sci* 1964;124:83.
- [27] Epple M. *J Therm Anal* 1995;45:1265.
- [28] Gehrke R, Riekel C, Zachmann HG. *Polymer* 1989;30:1582.